

Hybrid approach utilizing unmanned aerial vehicle and unmanned surface vehicle to assess the map of chlorophyll-a in a stream

Eunju Kim ¹, Sook-Hyun Nam ¹, Jae-Wuk Koo ¹ and Tae-Mun Hwang ^{1,2*}

¹. Korea Institute of Civil Engineering and Building Technology, 283 Goyangdar-Ro, Ilsan-Gu, Goyang-Si, Gyeonggi-Do 411-712, Republic of Korea; kej@kict.re.kr; fpnsh@kict.re.kr; koojaewuk@kict.re.kr; taemun@kict.re.kr

* Correspondence: taemun@kict.re.kr; Tel.: +82-31-910-0741+82-31-910-0291 (F.L.)

Abstract : The current study investigated the use of two-dimensional spatial distribution mapping representing the chlorophyll-a level in a river generated via an unmanned aerial vehicle (UAV) and an unmanned surface vehicle (USV). A domestically developed UAV (Remo-M, Uconsystem Inc., Korea) and a USV developed by our research team were used to collect data from the Nae Seong stream in Korea. An adaptation of the “Data Cleaner” tool was developed and used for USV data processing and analysis. The operation of the autonomous USV was successful. Four previously described indices for quantifying algal blooms in rivers were utilized to create chlorophyll-a images, the normalized difference vegetation index (NDVI), the normalized green red difference index, the green normalized difference vegetation index (GNDVI), and the normalized difference red edge index. The suitability of the linear regression analysis of the correlation between the spectral indices obtained using the UAV and the *in situ* chlorophyll-a data obtained using the USV was evaluated with the coefficient of determination (R^2) at a significance level of $p < 0.001$. Infield application and

correlational analysis, the NDVI was strongly correlated with chlorophyll-a ($R^2 = 0.88$, $p < 0.001$), and the GNDVI was moderately correlated with chlorophyll-a ($R^2 = 0.74$, $p < 0.001$). The map of chlorophyll-a was successfully quantified using the UAV and USV hybrid platforms.

Keywords: aerial vehicle; algal bloom index; autonomous; chlorophyll-a mapping; GNDVI; NDVI; surface vehicle; unmanned

1. Introduction

Algal blooms are a natural phenomenon that occurs in water-based ecosystems in response to environmental factors such as nutrition, light, water temperature, and wind speed [1]. Harmful algal blooms can cause substantial water quality problems that persist in rivers, lakes, and reservoirs [2-4]. Accordingly, monitoring algae in rivers, lakes, and other freshwater bodies is emerging as an increasingly critical issue. Of the various types of algae, blue-green algae is of particular concern given the potential existence of toxins within it, necessitating a fundamental solution for its reduction to avoid economic and social problems [5,6]. Because green algae exhibits repeated cycles of growth and death depending on environmental conditions such as light (solar radiation), water temperature, nutritional salts (nitrogen, phosphorus), and duration of residence, the data pertaining to green algae hot-spots need to be collected quickly and frequently.

Chlorophyll-a (Chl-a) is one of the photosynthetic pigments contained in algae, and it has traditionally been used as an indicator of algal biomass via field sampling to monitor algal growth. Fixed chlorophyll-a sensors are currently installed in South Korea to monitor sites such as major water sources, rivers, and lakes by way of an automatic water quality monitoring network. Field sampling and assessment of algae is also conducted to monitor chlorophyll-a levels and measure algal biomass [7]. Monitoring via field sampling and

chlorophyll-a measurement can be problematic with regard to temporal and spatial resolution however, because the locations and/or compositions of large-scale algal outbreaks can change dramatically in a short time due to multiple ubiquitous factors such as rain and wind. In an effort to address this issue recent studies have investigated the use of unmanned aerial vehicles (UAVs) to monitor chlorophyll-a [8-13].

Because most images acquired by UAVs for analysis are taken from a distance of 50–200 m, atmospheric correction is not necessary and multispectral sensors have proven effective for environmental monitoring [14-18]. The estimation of chlorophyll-a levels via remote detection data combined with field measurement involves the use of various algorithms [19-23]. The normalized distribution vegetation index (NDVI) is one of many spectral indices [24] that has been used in this context [1, 11, 18].

In order to capture chlorophyll-a images using a UAV, field analysis must be performed in the target aquatic area in conjunction with UAV measurement. Field analysis requires data collection at various points of the target waterway. Traditionally a boat has been required to measure chlorophyll-a in a river that is difficult to reach from land, but this is time and labor intensive, and entails numerous associated limitations. It is therefore necessary to develop a mobile but less cumbersome technology for immediate water quality measurement in the field [25]. Unmanned surface vehicles (USVs) have been the subject of recent research and development. They are being used in a variety of research areas, including water quality monitoring, surveillance, underwater terrain mapping, and oceanography [26-34]. As well as ameliorating space and time constraints by automating data collection, autonomous USV technology can be conducive to improved chlorophyll-a and water quality monitoring methods [34,35].

To date few studies have investigated the development and application of USVs in conjunction with UAVs in the field for visual two-dimensional spatial distribution mapping of chlorophyll-a. In the current study UAV and USV hybrid platforms combining the UAV spectrum with field data derived from a USV were used to capture chlorophyll-a images and monitor chlorophyll-a in the N Nae Seong stream (N36.805, E128.695) in Korea. As well as the NDVI, the use of other spectral indices to estimate chlorophyll-a was investigated.

2. Materials and Methods

2.1. The UAV

The UAV (Remo-M by Uconsystem Inc., Korea) used in the study is shown in Figure 1. It has fixed wings with a wingspan of 70.8 inches, and weighs 3.4 kg. It is equipped with a brushless AXI 2826/10 motor (Model Motors LTD., Czechia) and an Aero-naut carbon propeller (Germany). Its maximum speed is 80 km/hour and it has a minimum operating distance of 8 km. A Sequoia multispectral camera (Parrot Cor., France), is mounted on the UAV. Four sensors in the camera create multispectral images in four spectral bands; green (550 nm), red (660 nm), red edge (735 nm), and near-infrared (NIR) (790 nm).

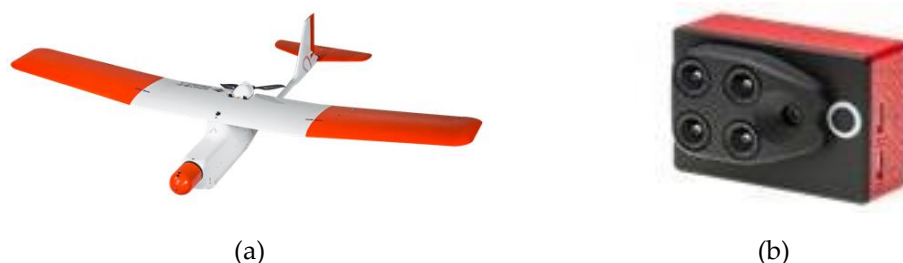


Figure 1. (a) The unmanned aerial vehicle (Remo-M) used in the study, and (b) its camera (Sequoia).

2.2. The USV

The USV used in the study was developed by our research team specifically for monitoring chlorophyll-a in the N stream, and it is shown in Figure 2. It is 1.3 m long, weighs

approximately 10 kg, and can operate at a maximum speed of 18 km/hour. The communication distance is 2 km or more, and the communication frequency is 2.400–2.483 GHz. In addition to a general camera sensor, an echo sound apparatus for measuring the depth of the river, and a Lidar sensor to prevent collisions, AlgaeChek Ultra (Modern Water, England) is installed for the measurement of chlorophyll-a. The water quality sensor is mounted at a location on the vehicle that is not affected by the propeller. The location receiving system consists of the global navigation satellite system L1 (GNSS) and a satellite-based augmentation system-class receiver of 5 Hz or higher. An autonomous navigation program is used to set the unmanned travel route. The main operation modes and functions are autonomous route operation, point navigation, and automatic return. The maximum operation time is approximately 5 hours. The water quality sensor and location data are synchronized with the flight control computer via a parsing protocol, and are stored in real time. Chlorophyll-a levels are recorded in the sensor in $\mu\text{g/L}$. The architecture of the USV system is shown in Figure 3.



Figure 2. The unmanned surface vehicle used in the study.

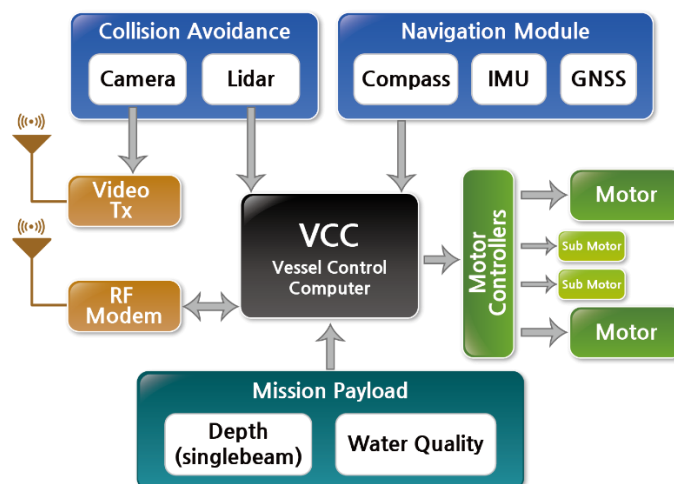


Figure 3. The architecture of the unmanned surface vehicle used in the study.

2.3. Study area

The UAV and USV were configured for field application targeting the N River (Figure 4). The N River is of interest because algal blooms occur there every year. The altitude of the UAV takeoff point was 150 m. Data were collected from a 3.2 km section during a single 15-minute flight. The flight commenced at approximately 8 am. To ensure lateral overlap of $\geq 65\%$ and longitudinal overlap of $\geq 75\%$ the images were taken in four strips at an altitude of 150 m. The wind speed during the flight was 0–10.8 km/hr.

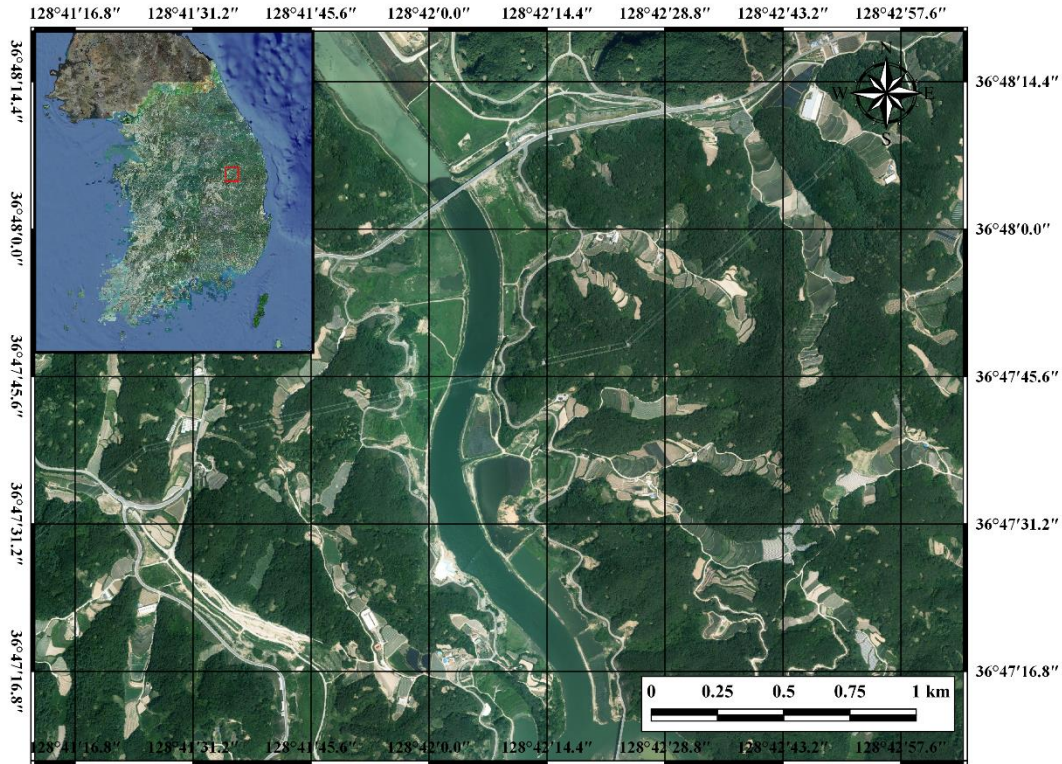


Figure 4. The study area (N River).

The entire 15-minute flight covering the 3.2 km section was photographed, with the camera set at 60-m strip intervals and a shooting interval of 2 seconds. For image identification, 15 ground control points were installed around the site before the flight so that positional image displacement could be corrected. Calibrated reflectance panel images were taken before and after UAV take off to calibrate the reflection values of the index calculator. The USV continuously measured chlorophyll-a during autonomous operation within a $2.31 \times 0.10 \text{ km}^2$ area along the N River. The route width was 20 m and the operating speed of the USV was 1.6 km/hour.

2.4. Statistical analysis

The data obtained from the USV were statistically analyzed using software developed in this study. USV data outside the 10%–90% range were considered outliers. Histogram analysis was applied to the USV field data to set the frequency and segment range. The suitability of the linear regression analysis of the correlation between the spectral index obtained using the UAV and the *in situ* chlorophyll-a data obtained using the USV was evaluated with the coefficient of determination (R^2) at a significance level of $p < 0.001$.

2.5. Chlorophyll-a spectral indices

The previously described multispectral indices that have been used as indicators of algal blooms in rivers [24] shown in Table 1 were used to generate UAV images of chlorophyll-a. The indices applied in the present study were the normalized difference vegetation index (NDVI), the normalized green red difference index (NGRDI), the green normalized difference vegetation index (GNDVI), and the normalized difference red edge index (NDREI).

Table 1. Spectral indices used for chlorophyll-a assessment in the current study.

Name	Derivation	Reference
------	------------	-----------

Normalized difference vegetation index (NDVI)	$(\text{NIR}^* - \text{red})/(\text{NIR} + \text{red})$	[34] [18]
Normalized green red difference index (NGRDI)	$(\text{green} - \text{red})/(\text{green} + \text{red})$	[36]
Green normalized difference vegetation index (GNDVI)	$(\text{NIR} - \text{green})/(\text{NIR} + \text{green})$	[37] [38]
Normalized difference red edge index (NDREI)	$(\text{NIR} - \text{red edge})/(\text{NIR} + \text{red edge})$	[39]

* NIR, near-infrared.

3. Results

3.1. UAV Image processing

A flowchart representing the UAV imaging and image analysis procedures used in the study is shown in Figure 5. The two main components were imaging performed by the UAV, and *in situ* water quality analysis performed by the USV. Spectral index was extracted from the image analysis data acquired via flight photogrammetry, chlorophyll-a estimations derived from USV field analysis were collated, and the combination of the two was used to generate a regression equation. R2 was then the estimated to determine whether to create chlorophyll-a images. If R2 in the regression equation is greater than or equal to 0.5 (i.e., “yes” in the flowchart), then chlorophyll-a is mapped. If R2 is less than 0.5 (i.e., “no”), the data are preprocessed again through data processing until the criterion is satisfied. The photographs were processed using orthomosaics, georeferenced digital surface models, and the two-dimensional mapping software Pix4D (Lausanne, Switzerland). At the initial processing stage external distortions caused by the UAV tilting and internal distortions caused by camera characteristics were corrected, and photo junction points were extracted via a scale-invariant key points algorithm [40]. To acquire a high quality ortho-image, the registration lines between two adjacent ortho-images and the mosaic registration lines must be checked. Due to the fact that all noise of the 3D point cloud can affect the editing of the ortho-image of the measured target area, image-taking activities were undertaken by maintaining the crosspoints at the same altitudes, and by maintaining the cross points of the measured subject area as much as possible. The ground sample distance of the data obtained from the stream was 19 cm. NDVI, NGRDI, GNDVI, and NDREI images were generated using green (550 nm), red (660 nm), red edge (735 nm), and near-infrared (790 nm) bands, which were four spectral bands of the sensor mounted on the UAV. NDVI values were extracted from the red (668 nm) band and the NIR (840 nm) band value calculation. NGDVI values were extracted from the red (668 nm) band and the green (550 nm) band value calculation. GNDVI values were extracted from the NIR (840 nm) band and the green (550 nm) band value calculation. NDREI values were extracted from the NIR (840 nm) band and red edge (735 nm) band value calculation. These values were calculated from -1 to +1.

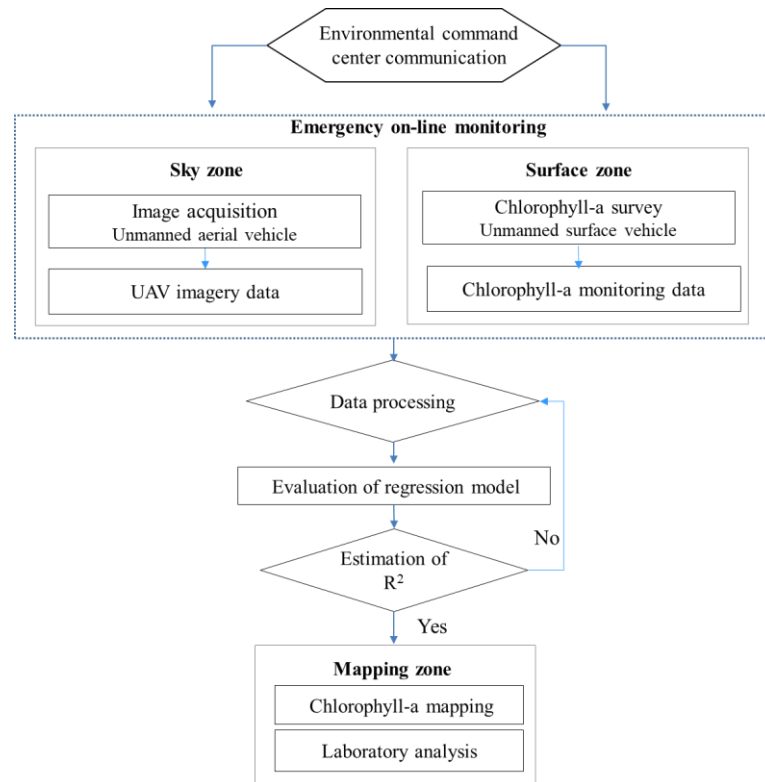


Figure 5. Flowchart representing the process used to map chlorophyll-a via a combination of an unmanned aerial vehicle and an unmanned surface vehicle.

3.2. USV data analysis

In situ chlorophyll-a data was obtained from the river by the USV as it travelled the route shown in Figure 6. The USV covered an area of 2.31 x 0.10 km² to acquire reliable data. The operating speed of the USV was set to 1.6 km/h, and it operated autonomously along the preprogrammed route.



Figure 6. The operator's remote field interface during examination of the N River.

Because raw data obtained from the USV are extensive, they must be processed prior to being compared with the UAV-derived image data. Exploratory data analysis is required for data processing [41]. To analyze the extensive raw data, an adapted version of the data analysis tool “Data Cleaner” was developed in this study. Data Cleaner is software written in the C# language and R. R is a programming language and free software environment for statistical computing (<https://www.r-project.org/>). In this study, it was programmed to compile and run on Windows. Data Cleaner sequentially conducts data-set verification, missing value processing, outlier removal, then feature engineering. Data Cleaner enables the user to visualize a histogram of the data obtained by the USV and the processed data within the target range. A histogram of the chlorophyll-a data obtained via the application of Data Cleaner is shown in Figure 7. In the present study values outside the 10%–90% range were deemed to be outliers. Figure 7 (a) shows a histogram of raw data obtained by the USV, and Figure 7 (b) shows a histogram of data within the 10–90 % range, in which the outliers were removed. The range of chlorophyll-a in the preprocessing of raw data was 0.2–48 $\mu\text{g/L}$, and the range of chlorophyll-a after data preprocessing was 4.0–29.0 $\mu\text{g/L}$. The number of data obtained by operating the USV was 242,818, and the number of data obtained by data processing was 194,258.

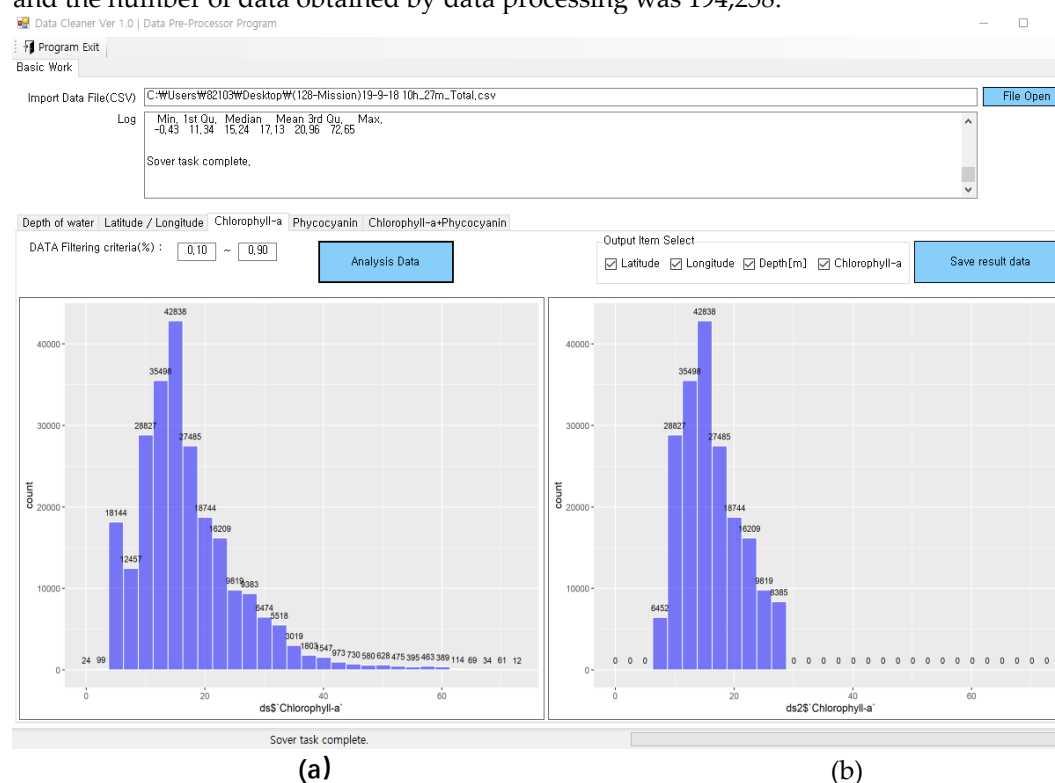


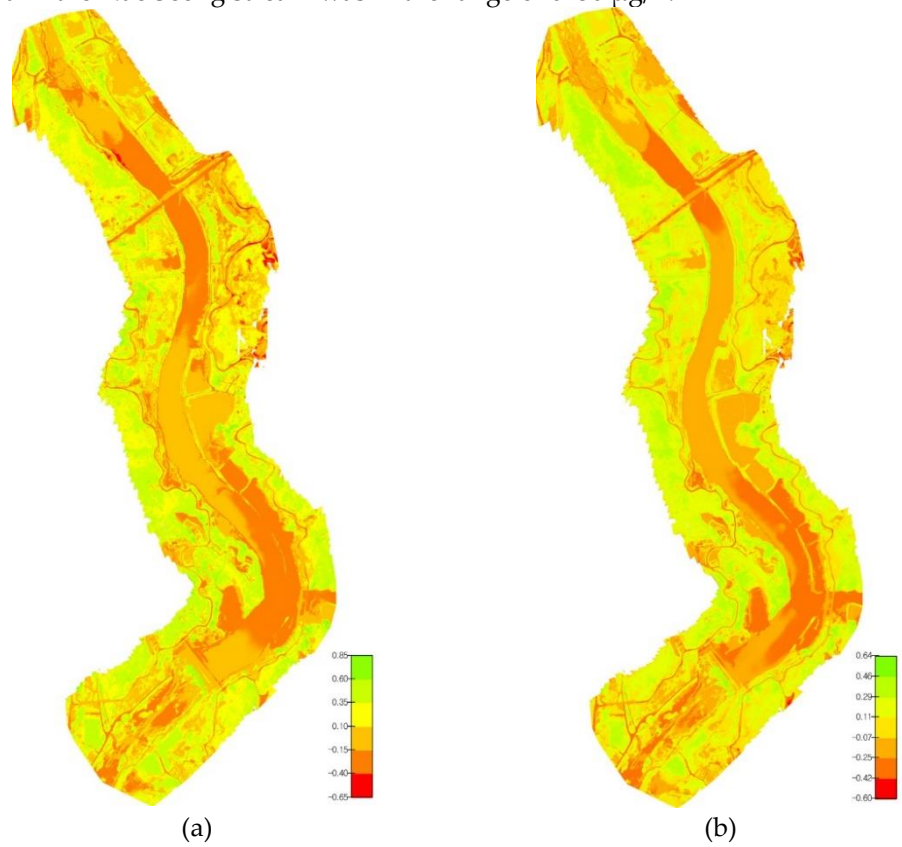
Figure 7. Exploratory data analysis tool developed in the study. (a) Histogram of USV raw data (b) Histogram of processed data within the 10%–90% range.

Using this tool, the chlorophyll-a measurements were segmented via histogram analysis, then the value of each segment was used for comparison with the spectral indices. The histogram range of chlorophyll-a was divided in 0.2 $\mu\text{g/L}$ intervals to classify the concentrations. Then, the mean of spectral indices corresponding to the range of chlorophyll-a showing frequencies was extracted and used.

3.3. Spectral indices analysis

In this study, we observed the four different indices (band ration algorithms), which were used to identify the chlorophyll-a, as indicators of algae bloom in the UAV images. These indices include NDVI, GNDVI, NDREI and NGRDI. The results of applying the four spectral indices are shown in Figure 8. The NDVI ranged from -0.3 to -0.08, the GNDVI from -0.35 to -0.16, the NDREI from -0.04 to 0.01, and the NGRDI from 0.02 to

0.13. The NDVI and the GNDVI showed lower values than the NDREI and the NGRDI. The results of correlational analysis between the four spectral indices and the *in situ* chlorophyll-a measurements obtained via the USV are shown in Figure 9. Chlorophyll-a was significantly correlated with the NDVI ($R^2 = 0.88$, $p < 0.001$) and the GNDVI ($R^2 = 0.74$, $p < 0.001$). It was not significantly correlated with the NDREI ($R^2 = 0.04$) or the NGRDI ($R^2 = 0.004$). As shown in Figure 10, the GNDVI and the NDVI have high correlations while the NGRDI shows the lowest correlation. These results demonstrate that although the NDVI reflects the characteristics of chlorophyll-a better than the GNDVI in the remote detection by UAV, the GNDVI can be also used to estimate the chlorophyll-a. In other words, chlorophyll-a can be estimated by identifying the green band, in addition to the red and NIR bands. Maps of chlorophyll-a derived using the NDVI and the GNDVI are shown in Figure 11. The legend for chlorophyll-a had a range of 0-120 $\mu\text{g/L}$ in both the maps using the NDVI and the GNDVI. Analyses using these indices indicated that the level of chlorophyll-a in the Nae Seong stream was in the range of 0–30 $\mu\text{g/L}$.



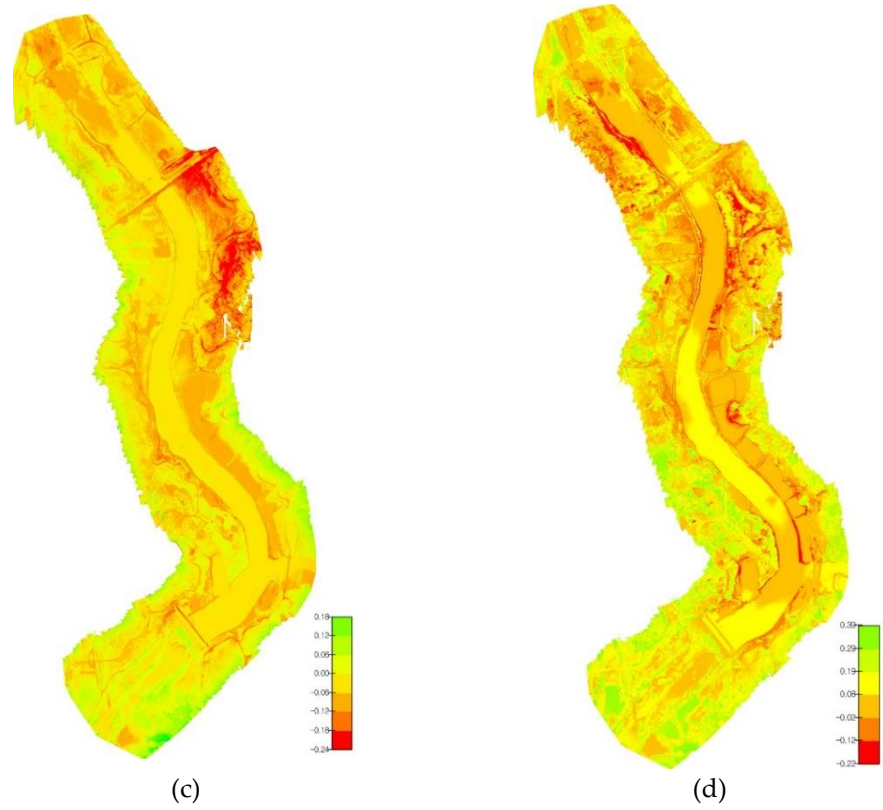


Figure 8. Results of image processing using each of the four spectral indices. (a) Normalized difference vegetation index. (b) Green normalized difference vegetation index. (c) Normalized difference red edge index. (d) Normalized green red difference index.

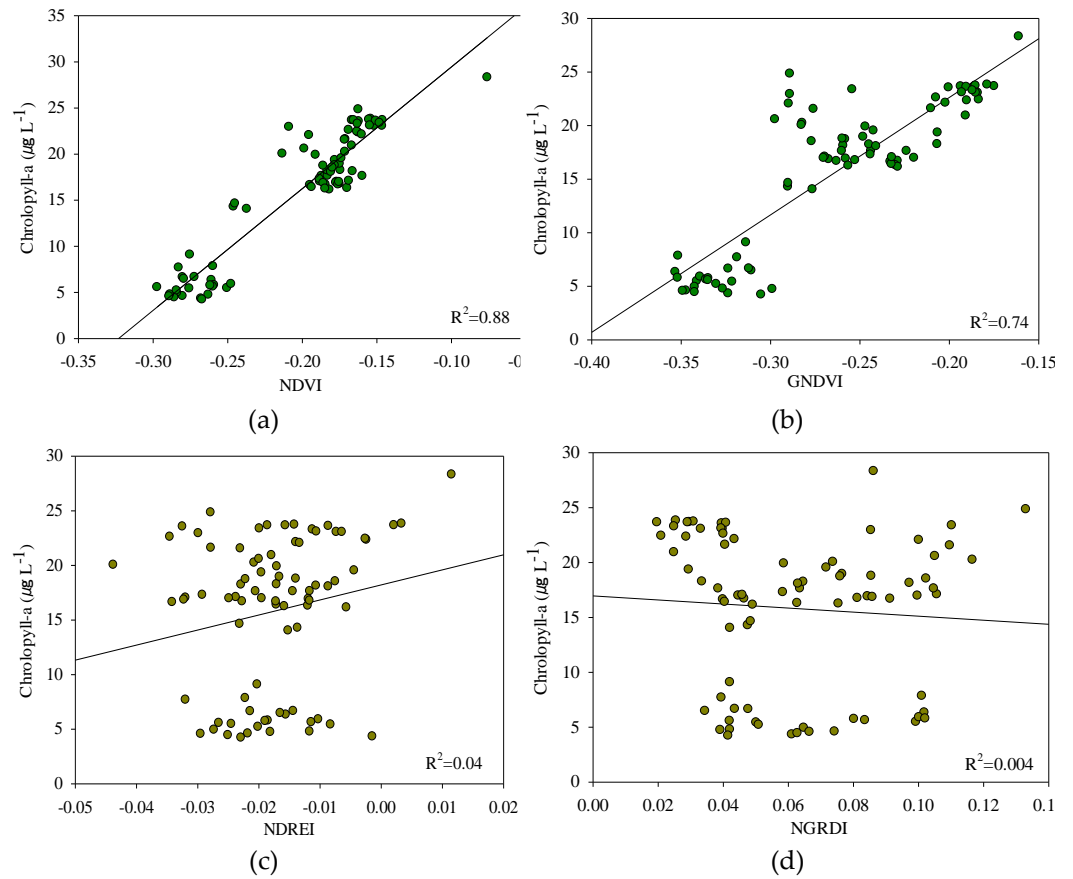


Figure 9. Regression analysis of the four spectral indices and chlorophyll-a. (a) Normalized difference vegetation index (NDVI). (b) Green normalized difference vegetation index (GNDVI). (c)

Normalized difference red edge index (NDREI). (d) Normalized green red difference index (NGRDI).

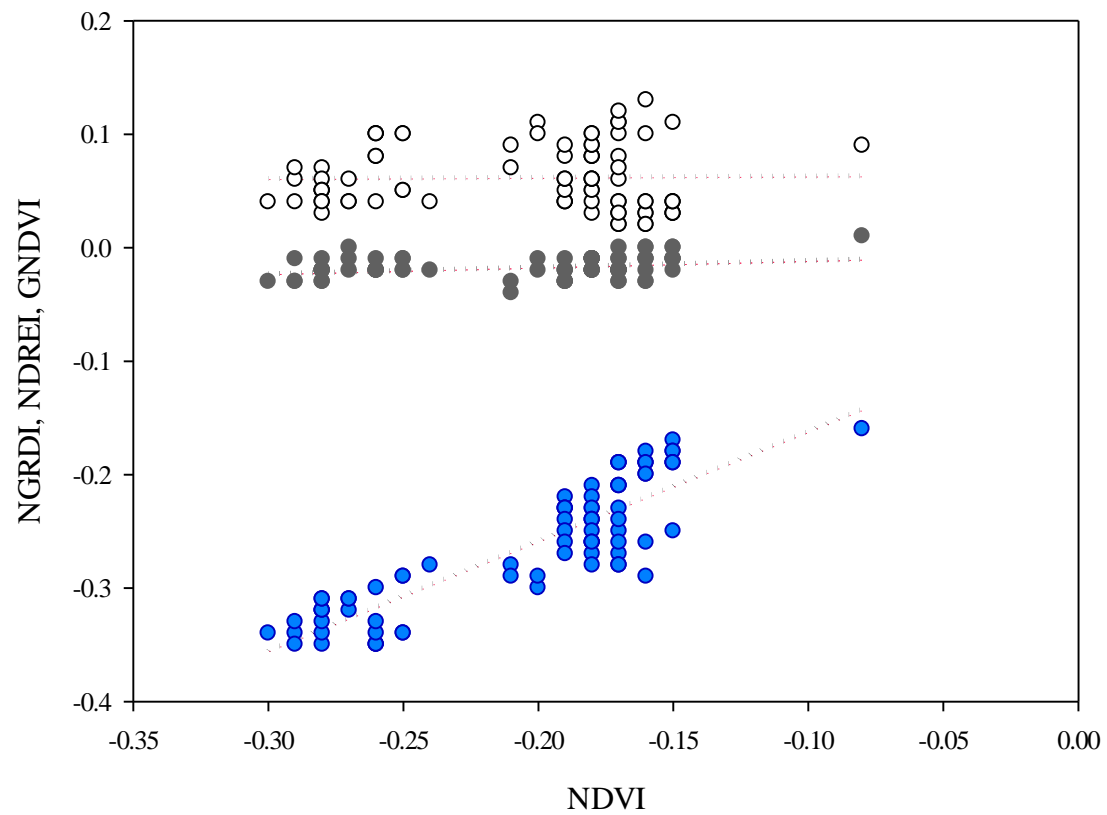


Figure 10. Correlation of the analysis between the NDVI and three vegetation index (GNDVI, NDREI, NGRDI).

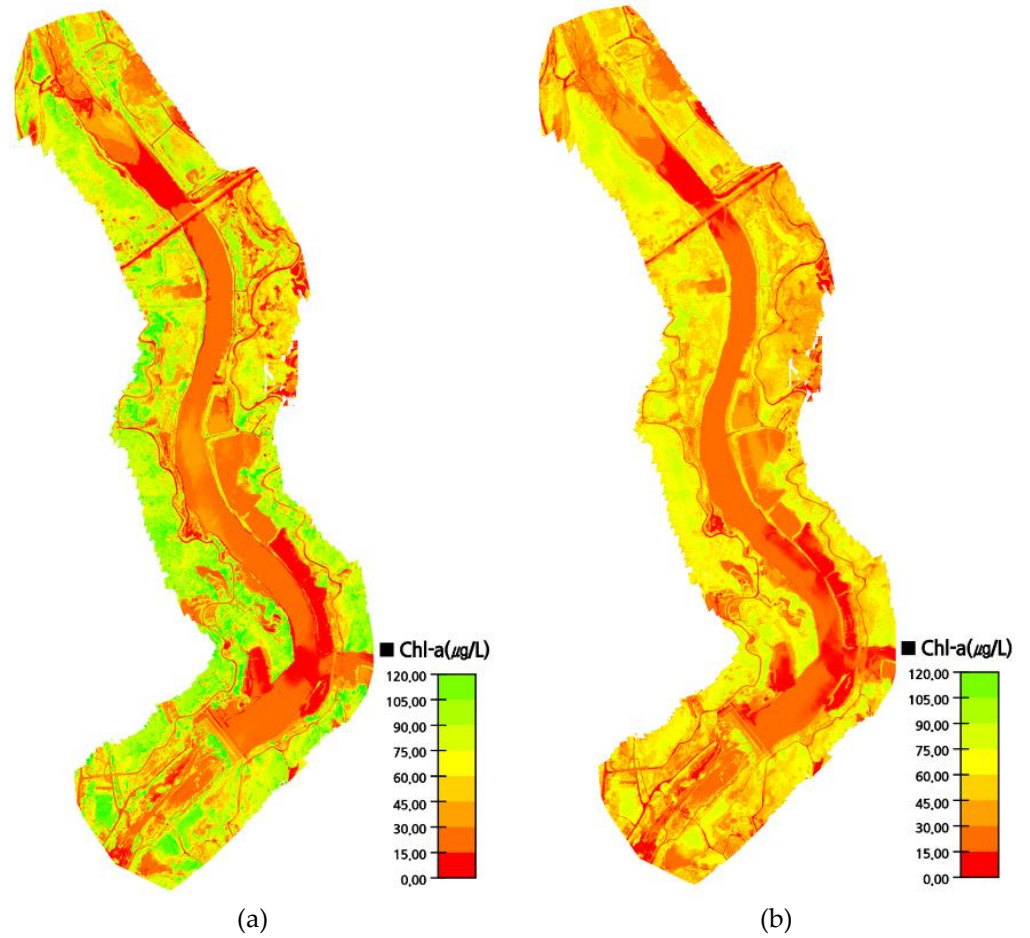


Figure 11. Chlorophyll-a maps derived using (a) the normalized difference vegetation index (NDVI) and (b) the green normalized difference vegetation index (GNDVI).

4. Discussion

UAV and USV hybrid platforms that use multispectral sensors and water quality sensors to detect and map chlorophyll-a as an indicator for algal blooms, they provide more reliable spatial information than UAV or USV alone and help identify specific algal species. The NDVI and the GNDVI were also reported to be effective indices in a previous study conducted on the detection of chlorophyll-a using vegetation indices and images obtained from a multispectral sensor-integrated UAV [24]. The results of the previous study revealed that the NDVI and the NGRDI had the highest and the lowest effectiveness, respectively, among the vegetation indices in the comparison between NDVI (Normalized Difference Vegetation Index), ENDVI (Enhance Normalized Difference Vegetation Index), NDREI (Normalized Difference RedEdge Index), NGRDI (Normalized Green-Red Difference Index), and GNDVI (Green Normalized Difference Vegetation Index) for waterside plants and floating plants of a certain period. Particularly, the NGRDI had a higher value on the water surface and was not useful for detection of aquatic plants. The NDVI and GNDVI, which showed the most apparent difference between aquatic vegetation and water surface, were reported to be the most effective for detecting aquatic plants [42]. Similar results were derived in this study when the vegetation indices were applied for detection of chlorophyll-a based on these results. In recent years, studies have been increasingly conducted using hyperspectral sensor to classify various types of phytoplankton. Although hyperspectral sensor is disadvantageous in terms of sensor weight and cost, there is an advantage in that higher spatial and temporal resolutions are provided compared to aircrafts or satellites. It is very important to collect and analyze many water-quality samples in order to visualize the chlorophyll-a element of river using vegetation indices with more reliable spectral resolution [43]. Furthermore, analysis results can be distorted due to wavelet distortion, solar reflection, shadow, and turbidity for subjects

with fast flow rate such as river. Regardless of which sensor is used, a large number of water quality data should be secured from the river having a characteristic of continuously fast flow rate for a same flight duration. This study used multispectral sensors of green (550 nm), red (660 nm), red edge (735 nm), and near-infrared (790 nm) bands. Furthermore, because chlorophyll-a shows different reflected signals depending on seasonal or visual appearance, the chlorophyll-a was measured at numerous points of the target waterbody using the USV during the flight time of UAV. In the results of analyzing the characteristics of the water quality data measured using the USV and various vegetation indices extracted from the multispectral images of UAV, the NDVI showed a very high correlation in terms of representing the characteristic of chlorophyll-a in the river. In addition to the NDVI, the GNDVI can be used to estimate chlorophyll-a because of identification of the green band, besides the red and the NIR bands, facilitates estimation of chlorophyll-a (Figure 10, Figure 11).

5. Conclusions

In order to capture chlorophyll-a images using a UAV, field analysis must be conducted in the target aquatic area in conjunction with UAV measurements. In the current study an autonomous USV and UAV hybrid system was developed to assess chlorophyll-a map. The use of the autonomous USV was successful because it facilitated the acquisition of two-dimensional visual chlorophyll-a data. The Data Cleaner tool was adapted and used in the analysis of USV data, and four types of spectral indices were applied to the UAV images to derive estimations of chlorophyll-a concentrations. The chlorophyll-a maps thus derived indicated that both the NDVI and the GNDVI were useful. Increased use of autonomous USVs to monitor water quality and chlorophyll-a concentrations is expected in the future.

Author Contributions: The following statements should be used “Project administration and conceptualization, T-M.; methodology, E.J., S-H.; software, E.J., S-H.; J-W. performed the field UAV and USV administration. All authors have read and agreed to the published version of the manuscript.

Funding: This study was funded by the major project of the Korea Institute of Civil Engineering and Building Technology (KICT) (grant number 20200044-001).

Acknowledgments: I would like to thank Uconsystem Incorporation and Hojung Solutions for their joint participation in this study.

Conflicts of Interest: The authors declare no conflicts of interest.

References

1. Van der Merwe, D.; Price, K.P. Harmful algal bloom characterization at ultra-high spatial and temporal resolution using small unmanned aircraft systems. *Toxins* **2015**, *27*, 1065–1078.
2. Hallegraeff, G.M.A. Review of harmful algal blooms and their apparent global increase. *Phycologia* **1993**, *32*, 79–99.
3. Preece, E.P.; Hardy, F.J.; Moore, B.C.; Bryan, M.A. Review of microcystin detections in Estuarine and Marine waters: environmental implications and human health risk. *Harmful Algae* **2017**, *61*, 31–45.
4. Shen, Q.; Zhu, J.; Cheng, L.; Zhang, Z.; Xu, Z. Enhanced algae removal by drinking water treatment of chlorination coupled with coagulation. *Desalination* **2011**, *271*, 236–240.
5. Teixeira, M.R.; Rosa, M. J. Comparing dissolved air flotation and conventional sedimentation to remove cyanobacterial cells of *Microcystis aeruginosa*: part I: the key operating conditions, *Separation and Purification Technology* **2006**, *52*, 84–94.
6. Figueiredo, D.R.; Azeiteiro, U.M.; Esteves, S.M.; Gon Alves, F.J.M.; Pereira, M.J. Microcystin-producing blooms—a serious global public health issue 1. *Ecotoxicology and Environmental Safety* **2004**, *59*, 151–163.
7. Gregor, J.; Marlek, B. Freshwater phytoplankton quantification by chlorophyll-a: a comparative study of in vitro, in vivo and in situ methods. *Water Research* **2004**, *38*, 517–522.
8. Watanabea, Y.; Kawaharab, Y. UAV photogrammetry for monitoring changes in river topography and vegetation. *Procedia Engineering* **2016**, *154*, 317–325.
9. Flynn, K.F.; Chapra, S.C. Remote sensing of submerged aquatic vegetation in a shallow non-turbid river using an

unmanned aerial vehicle. *Remote Sensing* **2014**, *6*, 12815-12836.

10. Pajares, G. Overview and current status of remote sensing applications based on unmanned aerial vehicles (UAVs), *Photogrammetric Engineering & Remote Sensing* **2015**, *81*, 4, 281-329.

11. Su, T.C.; Chou, H.T. Application of multispectral sensors carried on unmanned aerial vehicle (UAV) to trophic state mapping of small reservoirs: a case study of Tain-Pu reservoir in Kinmen, Taiwan. *Remote Sensing* **2015**, *7*(8), 10078–10097.

12. Zaman, B.; Jensen, A.; Clemens, S.R.; McKee, M. (2014) Retrieval of spectral reflectance of high resolution multispectral imagery acquired with an autonomous unmanned aerial vehicle AggieAir. *Photogrammetric Engineering & Remote Sensing* **2014**, *80*(12), 1139–1150.

13. Becker, R.H.; Sayers, M.; Dehm, D.; Shuchman R.; Quintero, K.; Bosse, K.; Sawtell, R. Unmanned aerial system based spectroradiometer for monitoring harmful algal blooms: A new paradigm in water quality monitoring. *Journal of Great Lakes Research* **2019**, *45*, 444–453.

14. Zarco-Tejada, P.J.; González-Dugo, V.; Berni, J.A.J. Fluorescence, temperature and narrow-band indices acquired from a UAV platform for water stress detection using a micro-hyperspectral imager and a thermal camera. *Remote Sensing of Environment* **2012**, *117*, 322-337.

15. Richardson, L.L. Remote sensing of algal bloom dynamics. *BioScience* **1996**, *46*(7), 492-501.

16. Aguirre-Gómez, R.; Salmerón-García, O.; Gómez-Rodríguez, G.; Peralta-Higuera, A. Use of unmanned aerial vehicles and remote sensors in urban lakes studies in Mexico, *International Journal of Remote Sensing* **2017**, *38*, 2771–2779.

17. Tong, A.; He, Y. Estimating and mapping chlorophyll content for a heterogeneous grassland: Comparing prediction power of a suite of vegetation indices across scales between years. *ISPRS Journal of Photogrammetry and Remote Sensing*. **2017**, *126*, 146–167.

18. Mishra, S.; Mishra, D.R. Normalized difference chlorophyll index: A novel model for remote estimation of chlorophyll-a concentration in turbid productive waters. *Remote Sensing of Environment* **2012**, *117*, 394–406.

19. Choe, E.Y.; Lee, J. W.; Lee, J. K. (2011) Estimation of chlorophyll-a concentrations in the Nakdong River using high-resolution satellite image. *Korean Journal of Remote Sensing* **2011**, *27*, 5, 613–623.

20. Chen, L.; Tan, C.H.; Kao, S.J.; Wang, T.S. Improvement of remote monitoring on water quality in a subtropical reservoir by incorporating grammatical evolution with parallel genetic algorithms into satellite imagery. *Water Research* **2008**, *42*(1–2), 296-306.

21. Gitelson, A.A.; Dall’Olmo, G.; Moses, W.; Rundquist, D.C.; Barrow, T.; Fisher, T.R.; Gurlin, D.; Holz, J. A simple semi-analytical model for remote estimation of chlorophyll-a in turbid waters: Validation. *Remote Sensing of Environment* **2008**, *112*, 3582-3593.

22. Brezonik, P.; Menken, K.D.; Bauer, M. Landsat-based remote sensing of lake water quality characteristics, including chlorophyll and colored dissolved organic matter (CDOM). *The Lake and Reservoir Management* **2005**, *21* (4), 373–382.

23. Tebbs, E. J.; Remedios, J. J.; Harper, D. M. Remote sensing of chlorophyll-a as a measure of cyanobacterial biomass in Lake Bogoria, a hypertrophic, saline-alkaline, flamingo lake, using Landsat ETM+. *Remote Sensing of Environment* **2013**, *135*, 92–106.

24. Kislik, C.; Dronova, I.; Kelly, M. UAVs in support of algal bloom research: A review of current applications and future opportunities. *Drones* **2018**, *2*, 35.

25. Ferri, G.; Manzi, A.; Fornai, F.; Ciuchi, F.; Laschi, C. The HydroNet ASV, a small-sized autonomous catamaran for real-time monitoring of water quality: From design to missions at sea. *IEEE Journal of Oceanic Engineering* **2015**, *40*, 710–726.

26. Naeem, W.; Sutton, R.; Chudley, J. Soft computing design of a linear quadratic Gaussian controller for an unmanned surface vehicle. *Proceedings of 14th Mediterranean Conference on Control and Automation*, Ancona, Italy **2006**, pp. 1–6.

27. Demetillo, A.T.; Taboada, E.B. Real-time water quality monitoring for small aquatic area using unmanned surface vehicle. *Engineering Technology and Applied Science Research* **2019**, *9*, 3959–3964.

28. Arzamendia, M.; Espartza, I.; Reina, D.G.; Toral, S.L.; Gregor, D. Comparison of Eulerian and Hamiltonian circuits for evolutionary-based path planning of an autonomous surface vehicle for monitoring Ypacarai Lake. *Journal of Ambient Intelligence and Humanized Computing* **2019**, *10*, 1495–1507.

28. Manley, J.E. Unmanned maritime vehicles, 20 years of commercial and technical evolution. *OCEANS 2016 MTS/IEEE Monterey*, Monterey, USA, **2016**, *9*, pp. 19–23.

29. Bayat, B.; Crasta, N.; Crespi, A.; Pascoal, A.M.; Ijspeert, A. Environmental monitoring using autonomous vehicles: a survey of recent searching techniques. *Curr Opin Biotechnol* **2017**, *45*, 76–84.

30. Wiora, J.; Kozyra, A.; Wiora, A. Towards automation of measurement processes of surface water parameters by a remote-controlled catamaran. *Bulletin of the Polish Academy of Sciences Technical Sciences* **2017**, *65*, 351–359.
31. Fornai, F.; Ferri, G.; Manzi, A.; Ciuchi, F.; Bartaloni, F.; Laschi, C. An autonomous water monitoring and sampling system for small-sized ASVs. *IEEE Journal of Oceanic Engineering* **2017**, *42*, 5–12.
32. Mousazadeh, H.; Hamid, J.; Elham, O.; Farshid, M.; Ali, K.; Yousef, S.; Ashkan, M. Experimental evaluation of a hydrography surface vehicle in four navigation modes. *Journal of Ocean Engineering and Science* **2017**, *2*, 127–136.
33. Rabah, F.K.J.; Ghabayen, S.M.; Salha A.A. Effect of GIS interpolation techniques on the accuracy of the spatial representation of groundwater monitoring data in Gaza Strip. *Journal of Environmental Science and Technology* **2011**, *4*, 579–589.
34. Goldberg, S.J.; Kirby, J.T.; Licht, S.C. Applications of aerial multi-spectral imagery for algal bloom monitoring in Rhode Island. *SURFO Technical Report No. 16-01*. University of Rhode Island: South Kingstown, RI, USA, **2016**, p. 28.
35. Mantzafleri, N.; Psilovikos, A.; Blanta, A. Water quality monitoring and modeling in Lake Kastoria, using GIS. Assessment and management of pollution sources. *Water Resources Management* **2009**, *23*, 3221–3254.
36. Xu, F.; Gao, Z.; Jiang, X.; Shang, W.; Ning, J.; Song, D.; Ai, J. A UAV and S2A data-based estimation of the initial biomass of green algae in the South Yellow Sea. *Marine Pollution Bulletin* **2018**, *128*, 408–414.
37. Jang, S.W.; Yoon, H.J.; Kwak, S.N.; Sohn, B.Y.; Kim, S.G.; Kim, D.H. Algal bloom monitoring using UAVs imagery. *Advanced Science and Technology Letters* **2016**, *138*, 30–33.
38. Kim, H.M.; Yoon, H.J.; Jang, S.W.; Kwak, S.N.; Sohn, B.Y.; Kim, S.G.; Kim, D.H. Application of unmanned aerial vehicle imagery for algal bloom monitoring in river basin. *International Journal of Control and Automation* **2016**, *9*, 203–220.
39. Gitelson, A.; Merzlyak, M.N. Quantitative estimation of chlorophyll-a using reflectance spectra: Experiments with autumn chestnut and maple leaves. *Journal of Photochemistry and Photobiology B: Biology* **1994**, *22*, 247–252.
40. Lowe, G.D. Distinctive image features from scale-invariant keypoints. *International Journal of Computer Vision*, **2004**, *20*, 91–110.
41. Ghasri, M.; Maghreb, M. Factors affecting unmanned aerial vehicles' safety: a post-occurrence exploratory data analysis of drones' accidents and incidents in Australia. *Australasian Transport Research Forum 2019 Proceedings* 30 September–02 October, Canberra, Australia.
42. Song, B.; Park, K. Detection of aquatic plants using multispectral UAV imagery and vegetation index. *Remote sensing*, **2020**, *12*, 387.
43. Koparan, C.; Koc, A.B.; Privette, C.V.; Sawyer, C.B. In situ water quality measurements using an unmanned aerial vehicle (UAV) system. *Water*, **2018**, *10*, 264.